Cellular and Molecular Neurobiology https://doi.org/10.1007/s10571-026-01679-w

Article in Press

Role of Kinin B_2 Receptor Signaling in Astrocyte-driven Neuroinflammation

Received: 8 August 2025

Accepted: 20 January 2026

Published online: 29 January 2026

Cite this article as: Tavares M.R., Estrela G.R., Lavezo L. *et al.* Role of Kinin B_2 Receptor Signaling in Astrocyte-driven Neuroinflammation. *Cell Mol Neurobiol* (2026). https://doi.org/10.1007/s10571-026-01679-w

Mariana R. Tavares, Gabriel R. Estrela, Luana Lavezo, Juliene L. S. Silva, Ronaldo C. Araujo, Michael Bader & Frederick Wasinski

Role of Kinin B_2 Receptor Signaling in Astrocyte-Driven Neuroinflammation

Mariana R. Tavares[1#], Gabriel R. Estrela[2#], Luana Lavezo[1], Juliene L. S. Silva[1], Ronaldo C. Araujo[2], Michael Bader[3, 4, 5], Frederick Wasinski[1*]

[1] Department of Neurology and Neurosurgery, Federal University of Sao Paulo, Sao Paulo 04039-032, Brazil

[2] Department of Biophysics, Federal University of Sao Paulo, Sao Paulo 04039-032, Brazil

[3] Max-Delbrück Center for Molecular Medicine (MDC), Robert-Rössle-Str. 10, 13125 Berlin, Germany

[4] German Center for Cardiovascular Research (DZHK), Partner Site Berlin, 10117 Berlin, Germany

[5] Institute for Biology, University of Lübeck, Ratzeburger Allee 160, 23562 Lübeck, Germany

* Corresponding author: f.wasinski@unifesp.br

# M.R.T. and G.R.E. contributed equally to this work

Abstract

The kallikrein–kinin system (KKS) plays a key role in inflammatory responses, but its specific contribution to neuroinflammation remains to be fully elucidated. The bradykinin B_2 receptor (B_2R), a principal effector of the KKS, is widely expressed in both neuronal and glial cells in the rodent and human brain. In this study, we investigated the molecular contribution of B_2R to neuroinflammation using complementary *in vitro* and *in vivo* models. Lipopolysaccharide (LPS) stimulation significantly upregulated B_2R mRNA expression in primary astrocyte cultures and in the cortical tissue of wild-type mice. Pharmacological blockade of B_2R in astrocytes markedly suppressed the LPS-induced proinflammatory gene expression. In contrast, B_2R antagonism in vivo resulted in only partial attenuation of the neuroinflammatory response. Together, these findings suggest cell type–specific roles for B_2R and underscore its key contribution to astrocyte-mediated neuroinflammation.

Keywords: neuroinflammation, bradykinin, kinin B_2 receptor, lipopolysaccharide, astrocytes

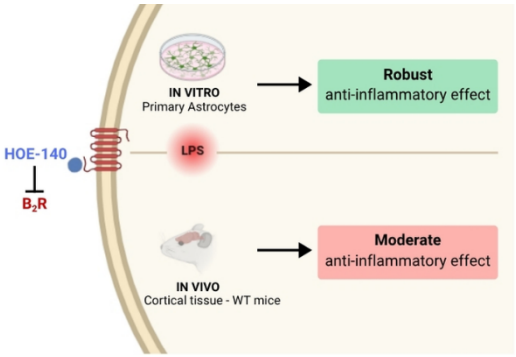

Graphical Abstract. B_2R antagonism highlights cell type–specific roles in neuroinflammation. B_2R pharmacological antagonism suppresses proinflammatory gene expression in astrocytes but shows limited *in vivo* efficacy, indicating differential functions across brain cell types.

Introduction

Neuroinflammation plays a central role in the pathophysiology of neurodegenerative disorders, including Alzheimer's disease, Parkinson's disease, and multiple sclerosis. Within the central nervous system (CNS), this process is mediated by resident glial cells—primarily microglia and astrocytes—which secrete cytokines and chemokines in response to intrinsic or extrinsic stimuli (Skrzypczak-Wiercioch and Sałat 2022). Under physiological conditions, glial cells contribute to key functions such as brain development, synaptic regulation, neuromodulation, and preservation of the blood–brain barrier (BBB). Nonetheless, when exposed to harmful stimuli—including infection, traumatic brain injury, cancer, or stroke—these cells undergo functional changes, adopting a proinflammatory profile characterized by the release of cytokines and reactive oxygen species aimed at limiting tissue damage and restore CNS homeostasis (Skrzypczak-Wiercioch and Sałat 2022).

The kallikrein-kinin system (KKS) is a proteolytic cascade that is well recognized for its activation under inflammatory conditions. It comprises both plasma and tissue kallikreins—enzymes responsible for the hydrolysis of high- and low-molecular-weight kininogens (HMWK and LMWK), resulting in the production of kinins, specifically bradykinin (BK) and kallidin (Lys-BK), respectively. These kinins are subsequently degraded by kininases, such as carboxypeptidases M and N as well as angiotensin-converting enzyme (ACE-I), into either inactive fragments or biologically active carboxy-terminally truncated peptides—des-Arg^9-BK and des-Arg^{10}-kallidin (Dutra 2017). These active metabolites are released at sites of tissue injury, where they function as potent inflammatory mediators by binding to two G protein-coupled receptors: the kinin B_1 and B_2 receptors (Sriramula 2020).

The kinin B_1 receptor (B_1R) is typically inducible, with its expression significantly upregulated in response to tissue injury or exposure to bacterial endotoxins such as lipopolysaccharide (LPS) (Prado et al. 2002), highlighting its critical role in inflammation. The truncated kinins des-Arg^9-BK and des-Arg^{10}-kallidin exhibit high affinity for B_1R (Dutra 2017). In contrast, the B_2 receptor (B_2R) is constitutively expressed under physiological conditions and is preferentially activated by intact BK and kallidin (Regoli and Barabé 1980). Activation of B_1R and B_2R triggers various cellular responses, including the release of prostaglandins and nitric oxide (NO), as well as the activation of signaling pathways such as nuclear factor-κB (NF-κB) and mitogen-activated protein kinases (MAPKs), both of which are commonly engaged in cellular stress responses (Dutra 2017).

B_2R is expressed in multiple regions of both rodent and human brains (Ongali et al. 2003; Mahabeer, Naidoo, and Raidoo 2000). However, its functional role within the CNS remains incompletely understood. While some studies report neuroprotective outcomes associated with B_2R activation (Toricelli et al. 2019; Nunes et al. 2020; Lemos et al. 2010), others suggest that enhanced B_2R signaling may exacerbate neuroinflammatory responses (Bicca et al. 2015; Dos Santos et al. 2008; Wehn et al. 2024). Given the central role of neuroinflammation in the progression of neurological disorders and the potential involvement of B_2R in this process, the present study aimed to investigate the molecular contribution of B_2R to neuroinflammation using both in vitro and in vivo approaches.

Methods

Mice

Postnatal day 1 to 2 (P1-P2) C57BL/6 mouse pups were used to isolate cortical cells for astrocytes culture. Eight-week-old male C57BL/6 mice were used for the in vivo assays. Mice were maintained in a 12-h light/dark cycle with ad libitum rodent chow (2.99 kcal/g; 9.4% kcal derived from fat; Nuvilab CR-1, Quimtia, Brazil). To induce acute neuroinflammation, LPS (Sigma-Aldrich, St. Louis, Missouri, USA #L2630) was injected intraperitoneally (5 mg/kg or 10 mg/kg as described). B_2R antagonist, HOE 140 (400 ug/kg i.p.; Sigma-Aldrich, St. Louis, Missouri, USA #138614-30-9) was injected 24h, 12h and 2h prior to LPS injection (Estrela et al. 2014). This multi-dose regimen was selected because HOE-140 has a short duration of action in vivo and undergoes rapid systemic clearance. Estrela et al. (2014) demonstrated that repeated pre-treatment injections are required to maintain sustained B2R antagonism during acute inflammatory challenges. Accordingly, we adopted the same approach to ensure continuous receptor blockade throughout the early LPS-induced inflammatory window. Three hours after LPS injection, the cortical region of the animals was carefully dissected. Mice were randomly assigned

to receive intraperitoneal Phosphate Buffered Saline (PBS; Control group, n = 4), LPS (LPS group, n = 4) and HOE-140 + LPS (HOE-140 + LPS group, n = 7) and investigators conducting the experiments were blinded to treatment allocation. The experimental procedures were approved by the Ethics Committee on the Use of Animals of the Universidade Federal de Sao Paulo.

Primary mouse astrocytes culture

To obtain adequate cell density, the cortices from two neonatal mouse pups were carefully isolated and dissected. The tissue was then dissociated and subjected to trypsinization (0.25% trypsin-EDTA, Gibco - Thermo Fisher Scientific, London, United Kingdom #25200-072), as previously described (Schildge et al. 2013). The resulting suspensions were centrifuged at 1200 rpm for 10 minutes. The pellet was resuspended in 10 mL of DMEM/F-12 Ham medium (Dulbecco's Modified Eagle Medium, Gibco - Thermo Fisher Scientific, London, United Kingdom #12400024) supplemented with 10% of fetal bovine serum (FBS; Gibco - Thermo Fisher Scientific, London, United Kingdom #12657-029). Cells were then seeded into 75 cm^2 culture flasks and maintained in an incubator at 37°C under a 5% CO_2 atmosphere until reaching semi-confluence (~90% of the total surface area). The culture medium was replaced every two days. Once 90% confluence was reached, the cells were considered ready for use in the proposed experiments (Figure 1A).

To assess the profile of inflammatory and anti-inflammatory gene expression in astrocytes, cells were seeded in 24-well plates and subjected to a starvation protocol in the presence or absence of HOE-140 (10 µM; Sigma-Aldrich, St. Louis, MO, USA; #138614-30-9). After 2 hours, the cells were stimulated with LPS (100 ng/mL; Sigma-Aldrich, #L2630) for various time points: 0h, 6h, 12h, and 24h. The RNA from the cells was subsequently extracted. Biological replicates: Control group, n = 5; LPS group, n = 6; HOE-140 + LPS group, n = 6.

Identification of astrocytes in the cell culture

Cells were cultured on 13 mm glass coverslips, fixed with 2% paraformaldehyde for 30 minutes, and subsequently washed with 1X PBS. Coverslips were then immersed in 0.1 M glycine solution (pH 7.4) for 30 minutes. Non-specific binding sites were blocked using a solution containing 5% FBS, 0.1% Triton X-100, 4% paraformaldehyde, and bovine serum albumin (BSA), followed by overnight incubation with primary antibody: anti-GFAP (Sigma-Aldrich, St. Louis, Missouri, USA #G9269; 1:500) at 4°C. After incubation, cells were washed and incubated for 1 hour at room temperature with secondary antibody Alexa Fluor 488 anti-rabbit (1:250 Thermo Fisher Scientific, London, United Kingdom;). Nuclei were counterstained with DAPI (Fluoromount-G, Electron Microscopic Sciences, Hatfield, PA). Photomicrographs were obtained using a confocal microscope (Leica TCS SP8)

at 40× magnification (400 µm). Data analyses were performed using LAS EZ software.

Calcium (Ca^{2+}) measurements after BK treatment of astrocytes

Intracellular [Ca^{2+}] fluctuations in astrocytes were assessed using the fluorescent dye Fluo-4 AM. Astrocytes were cultured in 25 mm glass coverslips. Cells were pre-incubated with Fluo-4 AM (5 µM; Invitrogen, Carlsbad, California, USA #F14201) and Pluronic F-127 (10%; Sigma-Aldrich, St. Louis, Missouri, USA #P2443) in fluorescence buffer (130 mM NaCl, 5.36 mM KCl, 1 mM $MgSO_4$, 1 mM Na_2HPO_4, 1.5 mM $CaCl_2$, 2.5 mM $NaHCO_3$, 1.5 mM albumin, 25 mM glucose, and 20 mM HEPES; pH 7.4) for 30 minutes. The fluorescence buffer was used either in the presence or absence of Ca^{2+}. Fluo-4 AM fluorescence was recorded at 494/506 nm using a real-time fluorescence microscope (Carl Zeiss LSM780) at 40× objective. Baseline fluorescence was acquired for 60 and 90 seconds, followed by stimulation with BK (1 µg; Sigma-Aldrich, St. Louis, Missouri, USA #B3259). Fluorescence signals were collected for 10 min, with a 3-second interval between images. Data analyses were performed using Zeiss Zen Lite software. Results are expressed as the peak fluorescence intensity of Fluo-4 AM (Zamarioli et al. 2024).

Quantitative Real-Time PCR

Total RNA was extracted from both astrocyte cells and mouse cortex using TRIzol reagent (Invitrogen, Waltham, USA). RNA concentration and purity were evaluated with an NanoDrop One spectrophotometer (Thermo Fisher Scientific, Waltham, USA). To eliminate any residual genomic DNA, samples were treated with RNase-free DNase I (Roche Applied Science, Penzberg, Germany). cDNA synthesis was carried out using 2 µg of total RNA, SuperScript II Reverse Transcriptase (Thermo Fisher Scientific, Waltham, USA), and random hexamer primers p(dN)6 (Roche Applied Science). Quantitative real-time PCR was conducted using the 7500TM Fast Real-Time PCR system (Applied Biosystems, Waltham, USA) and Power SYBR Green (Applied Biosystems) for fluorescence-based detection. Gene expression was analyzed using the 2^−ΔΔCt method, normalizing to *Actb* (β-actin) and *Ppia* (cyclophilin A) as reference genes for cortex and *Gapdh* for cells. The primers used are described in Table 1.

Table 1. Primer identification and sequences

Target gene	**Gene function**	**Foward primer**	**Reverse primer**
Actb (β-actin)	Reference gene	gctccggcatgtgcaaag	catcacaccctggtgccta
Bdkrb2 (B2R)	Bradykinin B2 receptor	ggtgctgaggaacaacgaga	cccaacacagcacaaagagc

	M2 macrophages		
Chil3 (YM1)	marker	cccctggacatggatgactt	agctcctctcaataagggcc
Gapdh	Reference gene	gctagccctggacatcgaga	ccccttctttggtgcttttgc
	Proinflammatory		
Il1b (IL-1β)	cytokine	gccacctttgacagtgatg	atgtgctgctgcgagatttg
	Antiinflammatory		
Il4r (IL-4R)	marker	cacagtgcacgaaagctgaa	atgggcacaagctgtggtag
	Proinflammatory		
Il6 (IL-6)	cytokine	tagtccttcctaccccaatttcc	ttggtccttagccactcctcc
	M2 macrophages		
Mrc1 (CD206)	marker	caaggaaggttggcatttgt	cctttcagtcctttgcaagc
Nos2 (iNOS)	Nitric oxide production	ctgctggtggtgacaagcacattt	atgtcatgagcaaaggcgcagaac
Ppia	Reference gene	cttcttgctggtcttgccattcc	tatctgcactgccaagactgagt
	Proinflammatory		
Tnf (TNF-α)	cytokine	gcctcttctcattcctgcttg	ctgatgagagggaggccatt

In addition to the expression of classical pro-inflammatory genes (TNFα, IL-1β, and IL-6), we also assessed the expression of markers associated with alternative macrophage activation and anti-inflammatory responses, such as CD206 (*Mrc1*) and YM1 (*Chil3*), as well as IL-4R, a regulatory receptor involved in modulating glial phenotype.

Statistics analysis

Sample size adequacy was determined a priori using G*Power 3.1 software, considering effect size = 0.8, statistical power (1-β = 0.8), and α = 0.05. Data normality was analyzed using the Shapiro-Wilk test and variance homogeneity was assessed prior to applying parametric tests. For datasets following a normal distribution, comparisons among multiple groups were performed using one-way analysis of variance (one-way ANOVA). When significant differences were detected, Tukey's post hoc analyses were conducted to identify pairwise differences. In cases of non-normal distribution, the non-parametric Kruskal-Wallis test was applied, followed by Dunn's post hoc analyses. Results are expressed as mean ± standard error of the mean (SEM), and statistical significance was defined as $p < 0.05$. All bar graphs display individual data points overlaid on the bars. All statistical analyses were carried out using GraphPad Prism software, version 8.0.1 (GraphPad Software,

San Diego, CA, USA). Group allocation was randomized, and data analysis was performed by an investigator blinded to group identity to minimize subjective bias. Complete statistical information and sample size of each figure are described in Supplementary Table 1.

Results

1. BK-Induced Intracellular Calcium Signaling in Primary Astrocytes Cultures

The experimental design used to obtain primary astrocyte cultures is illustrated in Figure 1A. To characterize the obtained cells, we performed immunofluorescence to assess the expression of glial fibrillary acidic protein (GFAP), a marker of astrocytes, and conducted an assay to evaluate changes in intracellular Ca^{2+} levels, given that bradykinin (BK) induces a transient increase in intracellular Ca^{2+} concentration through activation of B_2R (17). Figure 1B-D shows GFAP expression (green) in the culture, indicating that the cell population is predominantly composed of astrocytes. Figure 1E demonstrates the effect of BK on astrocytes, showing peaks of FLUO-4 fluorescence beginning at 60 seconds (black) and 90 seconds (red), coinciding with BK administration and indicating a BK-induced increase in intracellular [Ca^{2+}]. Figure 1F shows a representative image of astrocytes exposed to BK, illustrating increased Fluo-4 fluorescence intensity in nearly all cells following BK stimulation.

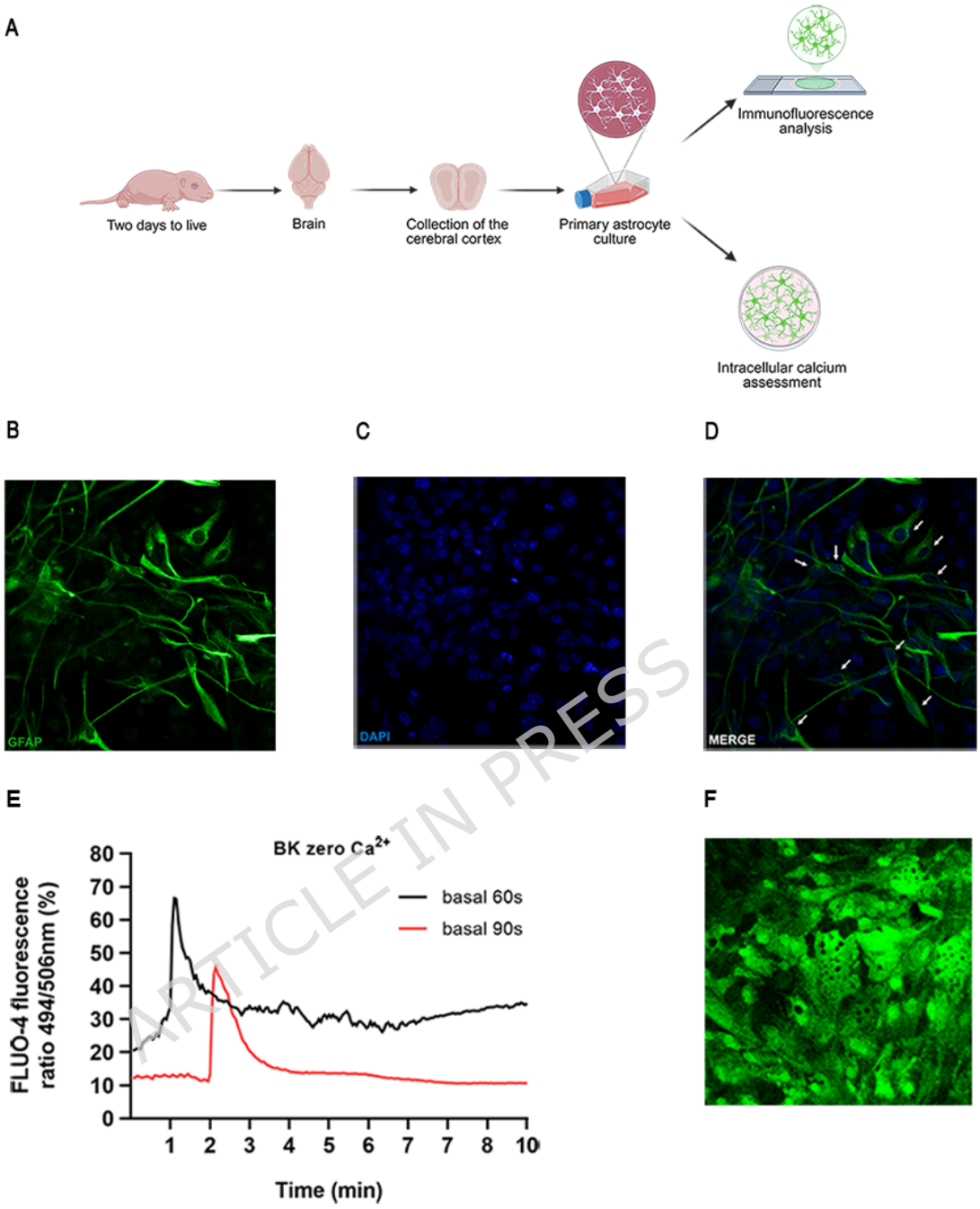

Fig. 1 Identification and characterization of primary astrocytes. A) Schematic representation of the experimental design used to establish primary astrocyte cultures. B, C, D) Representative images showing GFAP (green), DAPI (blue), and their colocalization (indicated by white arrows) in cultured astrocytes, scale bar: 400 µm. E) Representative amplitudes obtained from the Fluo-4 fluorescence ratio values (494/506 nm) in the basal state and with BK (1 µg) stimulus after 60 seconds (black line) and 90 seconds (red line), illustrating BK-evoked Ca^{2+} signaling. F) Representative confocal image of astrocyte cells stimulated with BK (1 µg) in the absence of Ca2+ in fluorescence buffer, illustrating calcium release from internal stores, scale bar: 400 µm

2. Pharmacological blockade of B_2R signaling inhibits LPS-induced inflammatory effects on gene expression in astrocytes

To investigate the role of B_2R in an inflammatory context in astrocytes, we conducted a time-course analysis of LPS treatment to determine the peak of LPS-induced B_2R gene expression. B_2R mRNA levels were assessed at 6h, 12h, and 24h following LPS stimulation. We observed that B_2R expression peaked at 6 hours post-LPS treatment (Figure 2A). Accordingly, all subsequent analyses in astrocytes were performed 6 hours after LPS exposure, with or without a 2-hour pretreatment with HOE-140 (Figure 2B). LPS treatment significantly increased the expression of all analyzed inflammatory markers in astrocytes, including TNF-α (Figure 2C), IL-1β (Figure 2D), IL-6 (Figure 2E) and iNOS (Figure 2F). This effect was completely abolished by blocking B2R signaling with HOE-140 (Figures 2C-F). Moreover, the absence of B_2R signaling in astrocytes resulted in increased expression of the anti-inflammatory gene YM1 (Figure 2H). Therefore, we conclude that blocking B_2R signaling in astrocytes was effective in reducing the intensity of LPS-induced inflammation by modulating the expression of pro-inflammatory markers and, to a lesser extent, promoting the expression of anti-inflammatory genes (Figures 2H and 2I).

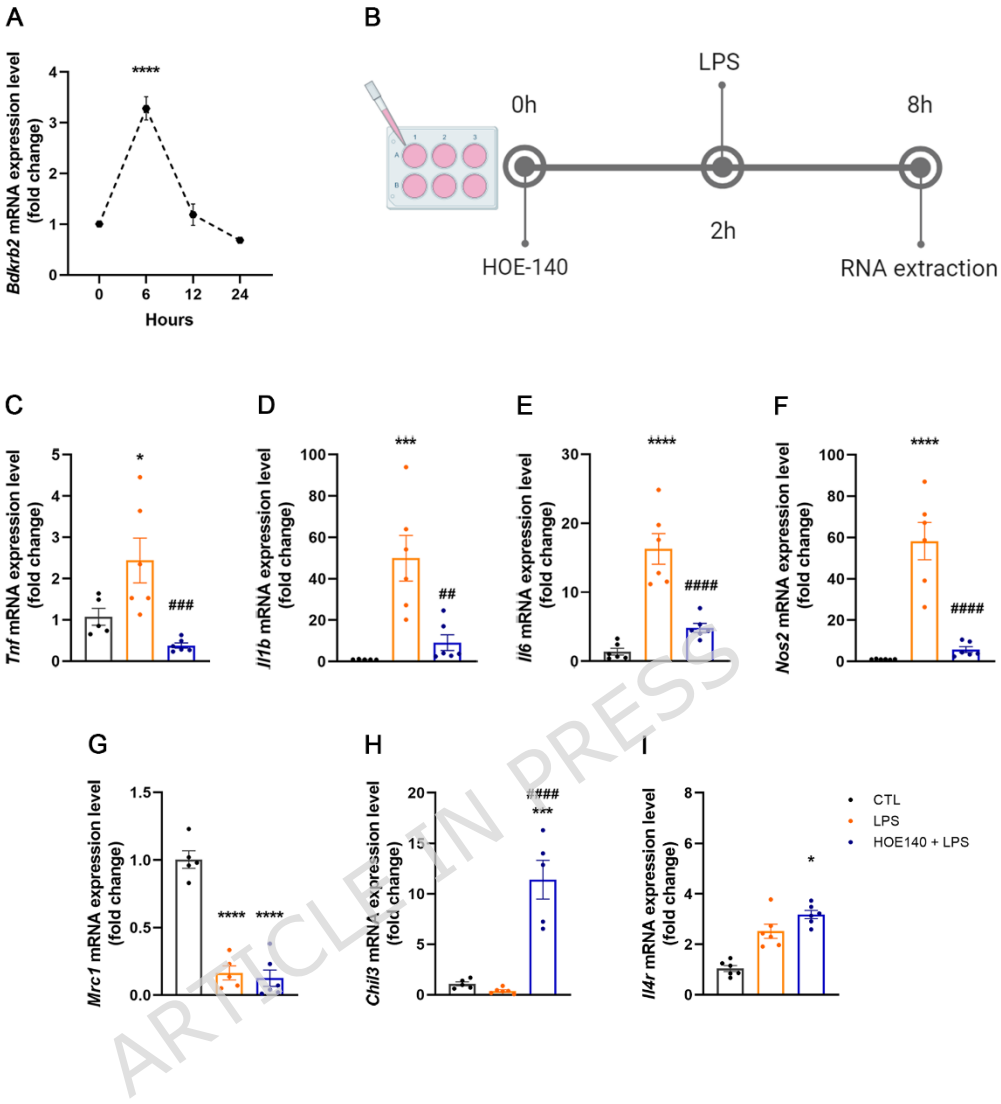

Fig. 2 Pharmacological blockade of B_2R inhibits LPS-induced inflammatory effects on gene expression in astrocytes. (A) Time-course analysis of B_2R gene expression in astrocytes following treatment with LPS (100 ng/mL) for 6, 12 or 24 hours (n = 5-6). (B) Schematic illustration of the experimental design used for evaluate the effects of HOE-140 (10 µM) and LPS (100 ng/mL) induced inflammation in astrocyte culture. (C-F) Relative mRNA expression of pro-inflammatory markers (TNF-α, IL-1β, IL-6, iNOS) in astrocytes treated with LPS alone (100 ng/mL) or in combination with HOE-140 (10 µM); (n = 6). (G- I) Expression of anti-inflammatory markers (CD206, YM1, IL-4R) under the same treatment conditions (n = 5-6). Data are expressed as mean ± SEM. * $p<0.05$; *** $p<0.001$; **** $p<0.0001$ vs control group. ## $p<0.01$; ### $p<0.001$; #### $p<0.0001$ vs LPS group

3. Pharmacological blockade of B_2R signaling partially attenuates LPS-induced inflammatory gene expression in mouse cortical tissue

To evaluate the effects of pharmacological inhibition of B_2R signaling on neuroinflammation in vivo, adult mice were treated with either a moderate (5 mg/kg ip) or a high (10 mg/kg ip) dose of LPS. Although the moderate LPS dose has been reported to induce neuroinflammation in adult mice (Hoogland et al. 2015), we selected the higher dose for the subsequent experiments because only the 10 mg/kg treatment consistently induced a significant increase in B2R mRNA levels in the cortex of young adult mice (Figure 3A). This higher dose is used in the literature to model acute systemic inflammation capable of triggering central nervous system inflammatory cascades, including cytokine upregulation, microglial activation, and sickness behavior (Hoogland et al. 2015; Bhaskar et al. 2010). Besides, data suggest that LPS-induced neuroinflammation in rodents can require mg-range doses to elicit reliable cytokine induction and CNS inflammatory signaling (Catorce and Gevorkian 2016; da Silva et al. 2024; Fu et al. 2014). Therefore, 10 mg/kg LPS provides a physiologically relevant and reliably reproducible model of acute neuroinflammation, which is necessary to investigate the contribution of B2R signaling in this context.

Figure 3B illustrates the experimental design employed for the treatment of mice. HOE-140 was administered intraperitoneally three times prior to LPS injection, with 12- and 10-hour intervals between each administration. In contrast to the *in vitro* experiments, cortical tissue *in vivo* displays a rapid inflammatory response, with robust induction of cytokines and inflammatory mediators occurring within 1–3 h after systemic LPS administration (Qin et al. 2007; Lee et al. 2008). For this reason, cortical tissue was analyzed 3 hours after LPS treatment (Figure 3B).

Unlike the pronounced effect of LPS in astrocytes, its induction of inflammatory gene expression in the cortex was relatively modest (Figures 3C–F). TNF-α expression was unexpectedly elevated in the cortices of animals pretreated with HOE-140 compared to both the control and LPS groups (Figure 3C). Besides, HOE-140 had no significant effect on IL-1β gene expression relative to the LPS group (Figure 3D). On the other hand, HOE-140 effectively reduced the expression of the inflammatory markers IL-6 and iNOS, which were upregulated by LPS treatment in the cortex (Figures 3E and 3F). Additionally, HOE-140 pretreatment decreased cortical expression of the anti-inflammatory genes CD206, YM1, and IL-4R compared to the LPS group (Figures 3G–I). Therefore, we conclude that the blockade of B2R signaling in vivo is less effective in suppressing the LPS-induced exacerbated inflammatory gene expression profile than its direct effect on astrocytes.

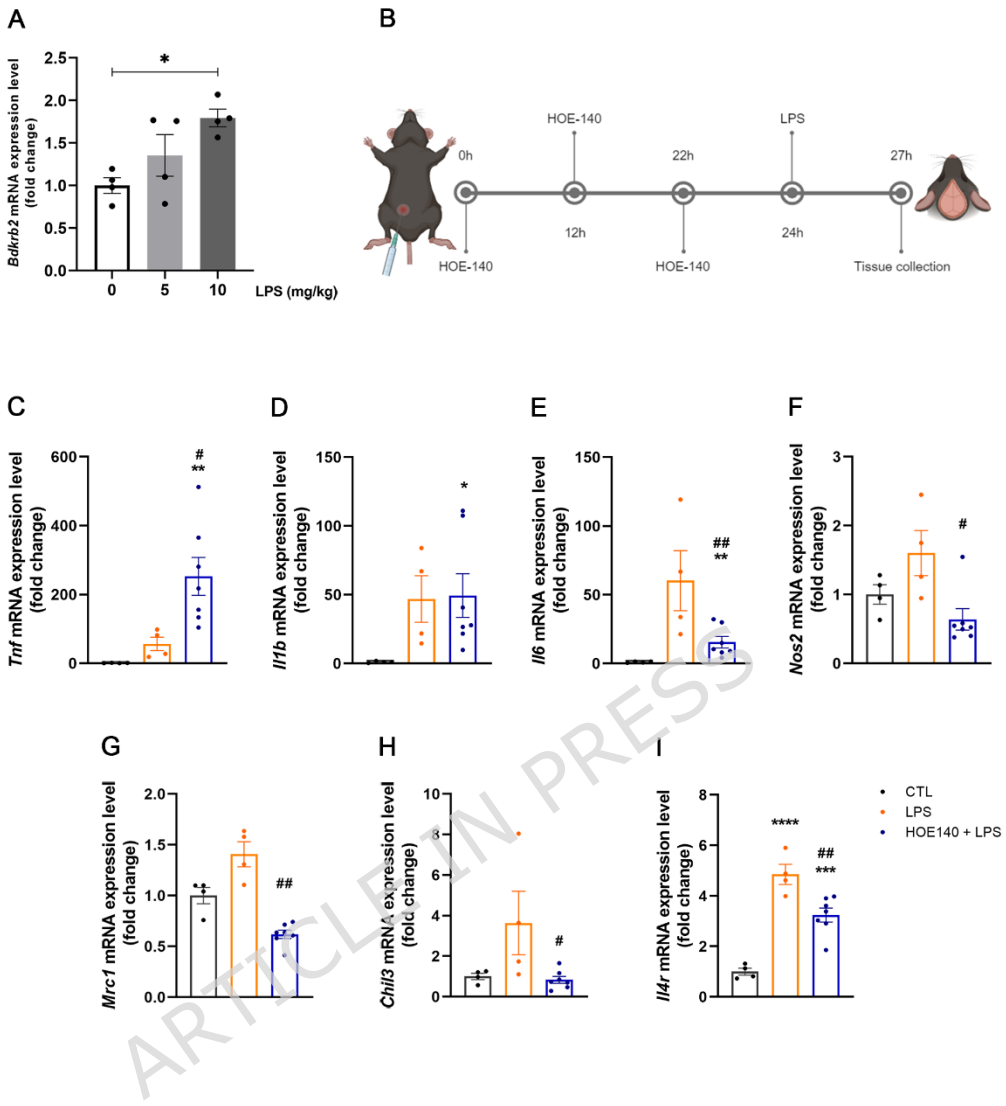

Fig. 3 Pharmacological blockade of B_2R partially attenuates LPS-induced inflammatory gene expression in mouse cortical tissue. (A) B_2R gene expression in the cortical tissue of mice intraperitoneally treated with two doses of LPS (5 and 10 mg/kg), compared to the control group (n = 4/group). (B) Schematic illustration of the experimental design used for treating animals with HOE-140 (400 ug/kg i.p.) and LPS (10 mg/kg i.p.). (C-F) Relative expression of pro-inflammatory markers (TNF-α, IL-1β, IL-6, iNOS) in the cortex of mice treated with LPS alone (10 mg/kg i.p.) or in combination with HOE-140 (400 ug/kg i.p.); (n = 4-7). (G-I) Expression of anti-inflammatory markers (CD206, YM1, IL-4R) in the same treatment groups (n = 4-7). Data are presented as mean ± SEM. * p<0.05; ** p<0,01; *** p<0.001; **** p<0.0001 vs control group. # p<0.05; ## p<0.01 vs LPS group

Discussion

In this study, we investigated the role of the kinin B_2 receptor (B_2R) in modulating the inflammatory response triggered by lipopolysaccharide (LPS) using both in vitro and in vivo models. Our findings indicate that B_2R signaling plays a key role in promoting pro-inflammatory gene expression in primary astrocyte cultures and, to a lesser extent, in the cortical tissue of adult mice. Furthermore, we demonstrate that pharmacological inhibition of B_2R with HOE-140 effectively suppresses LPS-induced inflammation in astrocytes, while eliciting partial anti-inflammatory effects in the cortex.

This pro-inflammatory profile is consistent with previously reported mechanisms. For instance, Levant et al. (2006) reported that bradykinin stimulation of B_2R in glial cells enhances prostaglandin E2 (PGE2) synthesis, especially under LPS-induced inflammatory conditions. In line with these findings, our model showed that activation of the LPS-B_2R axis upregulated inflammatory markers in astrocytes, and this response was significantly attenuated by B_2R antagonism. Collectively, these data support the hypothesis that B_2R functions as an amplifier of glial inflammatory responses and may represent a therapeutic target in conditions of exacerbated neuroinflammation.

Beyond its classical vascular role, B_2R signaling may also influence neuronal function through astrocyte-derived mediators. Liu et al. (2009) demonstrated that B_2R activation in astrocytes promotes glutamate release via reactive oxygen species (ROS) generation and activation of volume-sensitive outwardly rectifying (VSOR) Cl^- channels. Glutamate release may exacerbate neuronal excitability and contribute to excitotoxicity under sustained inflammatory conditions. Our findings complement this work by showing that B_2R activation also promotes cytokine expression in astrocytes, while its inhibition mitigates inflammatory responses. These complementary roles suggest that B_2R acts at the interface between neuroinflammation and synaptic dysfunction. Considering the pivotal role of glutamate in excitatory transmission and neuronal injury, targeting specific B_2R signaling in the astrocytes could offer a dual benefit: reducing inflammatory signaling and preserving neuronal integrity. Thus, selective B_2R inhibition emerges as a promising therapeutic strategy to limit glial-driven damage in neuroinflammatory contexts.

Extending beyond acute models, B_2R has also been implicated in chronic neuroinflammatory diseases. Consistent with our results, Dutra et al. (2013) showed that both pharmacological blockade and genetic deletion of B_2R reduce glial activation and pro-inflammatory cytokine expression in a murine model of multiple sclerosis (EAE). Although our study utilized an acute LPS-driven paradigm, both lines of evidence underscore the central role of B_2R signaling in shaping glial immune responses under diverse pathological conditions. Furthermore, the involvement of B_2R in astrocyte activation appears to be conserved across species

and immune challenges. For example, Kim et al. (2010) demonstrated that bradykinin triggers the expression of inflammatory cytokines in human astrocytes (1321N1 cell line) following zymosan stimulation, via MAPK and NF-κB activation. These findings align with our observations in murine primary astrocytes, in which HOE-140 reduced LPS-induced expression of TNF-α, IL-1β, IL-6 and iNOS. Such convergence strengthens the evidence for B_2R as a mediator of glial immune responses to various pro-inflammatory stimuli.

We also observed that inhibition of B_2R signaling, both *in vitro* and *in vivo*, resulted in decreased IL-6 and iNOS mRNA expression, consistent with previous studies showing that bradykinin stimulates IL-6 secretion and gene expression in astrocytes via NF-κB activation (Schwaninger et al. 1999), as well as the established mechanism by which bradykinin, through B2R activation, stimulates iNOS expression to promote nitric oxide production and subsequent vasodilation (Dutra 2017). These findings further support the involvement of B_2R in NF-κB–mediated cytokine production and position this receptor as a viable target for controlling astrocyte-driven inflammation in the CNS.

The anti-inflammatory effect of HOE-140 observed in the cortex of adult mice was less pronounced compared to that seen in isolated astrocytes. In contrast to the findings *in vitro*, HOE-140 treatment *in vivo* failed to reverse the LPS-induced upregulation of TNF-α and IL-1β, key proinflammatory cytokines involved in the acute phase of inflammation (Taishi et al. 2008)—corresponding to the specific time point at which cortical tissue was analyzed. Moreover, disruption of B_2R signaling reduced the expression of anti-inflammatory markers in vivo. These data may suggest a functional role for B_2R signaling in neurons, consistent with previously reported neuroprotective effects observed in neurons isolated from young mice (Toricelli et al. 2019). The discrepancy between the *in vitro* and *in vivo* findings may be explained by the cellular heterogeneity of the cortical environment, which comprises a variety of neuronal and glial cell types, each potentially responding differently to B_2R signaling. An important factor contributing to the discrepancy is that the cortex is a heterogeneous tissue composed of neurons, astrocytes, microglia, and endothelial cells, each expressing B2R and responding to LPS with distinct signaling dynamics. In purified astrocyte cultures, B2R antagonism directly reduces pro-inflammatory pathways; however, *in vivo*, neuronal B2R activation has been shown to attenuate excitotoxicity and limit inflammatory amplification (Sarit et al. 2012). Blocking this neuroprotective component may unmask or even potentiate microglial TNF-α production, explaining why TNF-α increases after HOE-140 treatment despite the attenuating effects observed *in vitro*. Likewise, IL-1β expression may be less sensitive to B2R blockade in a mixed-cell environment, where multiple regulatory circuits converge. These results reinforce the idea that the contribution of the kallikrein–kinin system (KKS) to neuroinflammation is highly

context-dependent, varying according to cell type, developmental stage, and the specific cellular milieu involved (Toricelli et al. 2019).

Importantly, several studies demonstrate that B2R activation can exert neuroprotective effects depending on stimulus intensity and cellular context. In models of ischemia and inflammatory injury, B2R signaling has been shown to reduce neuronal loss, modulate oxidative stress, and promote tissue recovery (Ji et al. 2017; Ji et al. 2019). These findings support the notion that B2R participates in homeostatic mechanisms that balance inflammatory signaling and neuronal survival, offering a plausible explanation for the region- and cell type–dependent transcriptional patterns observed in our study.

In addition, we investigated the role of B_2R signaling in an acute neuroinflammatory state in young adult mice. While our study focused on this specific context, previous research has demonstrated a neuroprotective role for B_2R in aging and neurodegenerative diseases, such as Alzheimer's disease (Caetano et al. 2015; Nunes et al. 2020; Ji et al. 2019), including improvements in certain cognitive parameters—which were not assessed in our model. Nonetheless, the effects of B_2R signaling in neurological disorders remain controversial, particularly concerning its function in neurons and glial cells, as thoroughly reviewed by Nokkari et al. (2018). Moreover, B2R signaling can engage multiple downstream pathways, such as ERK1/2–apelin/APJ or ERK1/2–NF-κB, which may play distinct roles in neuroprotection and neuroinflammation, respectively (Ji et al. 2019). Although the involvement of the kallikrein–kinin system (KKS) in neuroinflammation is well established, the specific contribution of each component requires further investigation to clarify the conflicting findings reported in the current literature. The use of available genetic models offers a promising strategy to dissect these complexities across different neuroinflammatory contexts. Alternatively, co-culture systems comprising neurons and glial cells offer a controlled in vitro environment to further investigate the role of the KKS in neuroinflammatory processes.

It is also important to note that no commercially available antibodies reliably detect B1R or B2R in mouse tissue, a limitation widely recognized in the kinin receptor field. This constraint restricts the feasibility of protein-level assays such as Western blot or immunohistochemistry, making qPCR analysis and pharmacological manipulation with a selective B2R antagonist (HOE-140) the most robust and reproducible approaches currently available to assess receptor involvement.

Taken together, our findings highlight the pivotal role of B_2R in astrocyte-driven neuroinflammation, reinforcing evidence from both acute and chronic models of CNS injury. Limiting the persistent activation of glial cells is crucial to prevent neuronal damage and, consequently, neurodegeneration (Qin et al. 2007). Our data identify B_2R as a potential therapeutic target, specifically in astrocytes, to mitigate this pathological process. Future studies are warranted to determine whether

targeting B_2R can attenuate long-term neuroinflammatory damage and preserve CNS homeostasis in disease models.

References

Bhaskar, K., M. Konerth, O. N. Kokiko-Cochran, A. Cardona, R. M. Ransohoff, and B. T. Lamb. 2010. 'Regulation of tau pathology by the microglial fractalkine receptor', *Neuron*, 68: 19-31.

Bicca, M. A., R. Costa, G. Loch-Neckel, C. P. Figueiredo, R. Medeiros, and J. B. Calixto. 2015. 'B_2 receptor blockage prevents Aβ-induced cognitive impairment by neuroinflammation inhibition', *Behav Brain Res*, 278: 482-91.

Caetano, A. L., K. E. Dong-Creste, F. A. Amaral, K. C. Monteiro-Silva, J. B. Pesquero, M. S. Araujo, W. R. Montor, T. A. Viel, and H. S. Buck. 2015. 'Kinin B2 receptor can play a neuroprotective role in Alzheimer's disease', *Neuropeptides*, 53: 51-62.

Catorce, M. N., and G. Gevorkian. 2016. 'LPS-induced Murine Neuroinflammation Model: Main Features and Suitability for Pre-clinical Assessment of Nutraceuticals', *Curr Neuropharmacol*, 14: 155-64.

da Silva, A. A. F., M. B. Fiadeiro, L. I. Bernardino, C. S. P. Fonseca, G. M. F. Baltazar, and A. C. B. Cristóvão. 2024. '"Lipopolysaccharide-induced animal models for neuroinflammation - An overview."', *J Neuroimmunol*, 387: 578273.

Dos Santos, A. C., E. Roffê, R. M. Arantes, L. Juliano, J. L. Pesquero, J. B. Pesquero, M. Bader, M. M. Teixeira, and J. Carvalho-Tavares. 2008. 'Kinin B2 receptor regulates chemokines CCL2 and CCL5 expression and modulates leukocyte recruitment and pathology in experimental autoimmune encephalomyelitis (EAE) in mice', *J Neuroinflammation*, 5: 49.

Dutra, R. C. 2017. 'Kinin receptors: Key regulators of autoimmunity', *Autoimmun Rev*, 16: 192-207.

Dutra, R. C., A. F. Bento, D. F. Leite, M. N. Manjavachi, R. Marcon, M. A. Bicca, J. B. Pesquero, and J. B. Calixto. 2013. 'The role of kinin B1 and B2 receptors in the persistent pain induced by experimental autoimmune encephalomyelitis (EAE) in mice: evidence for the involvement of astrocytes', *Neurobiol Dis*, 54: 82-93.

Estrela, G. R., F. Wasinski, R. F. Bacurau, D. M. Malheiros, N. O. Câmara, and R. C. Araújo. 2014. 'Kinin B2 receptor deletion and blockage ameliorates cisplatin-induced acute renal injury', *Int Immunopharmacol*, 22: 115-9.

Fu, H. Q., T. Yang, W. Xiao, L. Fan, Y. Wu, N. Terrando, and T. L. Wang. 2014. 'Prolonged neuroinflammation after lipopolysaccharide exposure in aged rats', *PLoS One*, 9: e106331.

Hoogland, I. C., C. Houbolt, D. J. van Westerloo, W. A. van Gool, and D. van de Beek. 2015. 'Systemic inflammation and microglial activation: systematic review of animal experiments', *J Neuroinflammation*, 12: 114.

Ji, B., B. Cheng, Y. Pan, C. Wang, J. Chen, and B. Bai. 2017. 'Neuroprotection of bradykinin/bradykinin B2 receptor system in cerebral ischemia', *Biomed Pharmacother*, 94: 1057-63.

Ji, B., Q. Wang, Q. Xue, W. Li, X. Li, and Y. Wu. 2019. 'The Dual Role of Kinin/Kinin Receptors System in Alzheimer's Disease', *Front Mol Neurosci*, 12: 234.

Kim, D., S. H. Cho, J. S. Kim, S. H. Jo, S. J. Lee, K. T. Kim, and S. Y. Choi. 2010. 'Human astrocytic bradykinin B(2) receptor modulates zymosan-induced cytokine expression in 1321N1 cells', *Peptides*, 31: 101-7.

Lee, J. W., Y. K. Lee, D. Y. Yuk, D. Y. Choi, S. B. Ban, K. W. Oh, and J. T. Hong. 2008. 'Neuro-inflammation induced by lipopolysaccharide causes cognitive impairment through enhancement of beta-amyloid generation', *J Neuroinflammation*, 5: 37.

Lemos, M. T., F. A. Amaral, K. E. Dong, M. F. Bittencourt, A. L. Caetano, J. B. Pesquero, T. A. Viel, and H. S. Buck. 2010. 'Role of kinin B1 and B2 receptors

in memory consolidation during the aging process of mice', *Neuropeptides*, 44: 163-8.

Levant, A., E. Levy, M. Argaman, and S. Fleisher-Berkovich. 2006. 'Kinins and neuroinflammation: dual effect on prostaglandin synthesis', *Eur J Pharmacol*, 546: 197-200.

Liu, H. T., T. Akita, T. Shimizu, R. Z. Sabirov, and Y. Okada. 2009. 'Bradykinin-induced astrocyte-neuron signalling: glutamate release is mediated by ROS-activated volume-sensitive outwardly rectifying anion channels', *J Physiol*, 587: 2197-209.

Mahabeer, R., S. Naidoo, and D. M. Raidoo. 2000. 'Detection of tissue kallikrein and kinin B1 and B2 receptor mRNAs in human brain by in situ RT-PCR', *Metab Brain Dis*, 15: 325-35.

Nokkari, A., H. Abou-El-Hassan, Y. Mechref, S. Mondello, M. S. Kindy, A. A. Jaffa, and F. Kobeissy. 2018. 'Implication of the Kallikrein-Kinin system in neurological disorders: Quest for potential biomarkers and mechanisms', *Prog Neurobiol*, 165-167: 26-50.

Nunes, M. A., M. Toricelli, N. M. Schöwe, H. N. Malerba, K. E. Dong-Creste, Dmat Farah, K. De Angelis, M. C. Irigoyen, F. Gobeil, T. Araujo Viel, and H. S. Buck. 2020. 'Kinin B2 Receptor Activation Prevents the Evolution of Alzheimer's Disease Pathological Characteristics in a Transgenic Mouse Model', *Pharmaceuticals (Basel)*, 13.

Ongali, B., M. M. Campos, G. Bregola, D. Rodi, D. Regoli, G. Thibault, M. Simonato, and R. Couture. 2003. 'Autoradiographic analysis of rat brain kinin B1 and B2 receptors: normal distribution and alterations induced by epilepsy', *J Comp Neurol*, 461: 506-19.

Prado, G. N., L. Taylor, X. Zhou, D. Ricupero, D. F. Mierke, and P. Polgar. 2002. 'Mechanisms regulating the expression, self-maintenance, and signaling-function of the bradykinin B2 and B1 receptors', *J Cell Physiol*, 193: 275-86.

Qin, L., X. Wu, M. L. Block, Y. Liu, G. R. Breese, J. S. Hong, D. J. Knapp, and F. T. Crews. 2007. 'Systemic LPS causes chronic neuroinflammation and progressive neurodegeneration', *Glia*, 55: 453-62.

Regoli, D., and J. Barabé. 1980. 'Pharmacology of bradykinin and related kinins', *Pharmacol Rev*, 32: 1-46.

Sarit, B. S., G. Lajos, D. Abraham, A. Ron, and F. B. Sigal. 2012. 'Inhibitory role of kinins on microglial nitric oxide and tumor necrosis factor-α production', *Peptides*, 35: 172-81.

Schildge, S., C. Bohrer, K. Beck, and C. Schachtrup. 2013. 'Isolation and culture of mouse cortical astrocytes', *J Vis Exp*.

Schwaninger, M., S. Sallmann, N. Petersen, A. Schneider, S. Prinz, T. A. Libermann, and M. Spranger. 1999. 'Bradykinin induces interleukin-6 expression in astrocytes through activation of nuclear factor-kappaB', *J Neurochem*, 73: 1461-6.

Skrzypczak-Wiercioch, A., and K. Sałat. 2022. 'Lipopolysaccharide-Induced Model of Neuroinflammation: Mechanisms of Action, Research Application and Future Directions for Its Use', *Molecules*, 27.

Sriramula, S. 2020. 'Kinin B1 receptor: A target for neuroinflammation in hypertension', *Pharmacol Res*, 155: 104715.

Taishi, P., L. Churchill, A. De, F. Obal, Jr., and J. M. Krueger. 2008. 'Cytokine mRNA induction by interleukin-1beta or tumor necrosis factor alpha in vitro and in vivo', *Brain Res*, 1226: 89-98.

Toricelli, M., S. R. Evangelista, L. R. Oliveira, T. A. Viel, and H. S. Buck. 2019. 'Neuroprotective Effects of Kinin B2 Receptor in Organotypic Hippocampal Cultures of Middle-Aged Mice', *Front Aging Neurosci*, 11: 168.

Wehn, A. C., I. Khalin, S. Hu, B. N. Harapan, X. Mao, S. Cheng, N. Plesnila, and N. A. Terpolilli. 2024. 'Bradykinin 2 Receptors Mediate Long-Term Neurocognitive Deficits After Experimental Traumatic Brain Injury', *J Neurotrauma*, 41: 2442-54.

Zamarioli, L. D. S., M. R. M. Santos, A. G. Erustes, V. M. Meccatti, T. C. Pereira, S. S. Smaili, M. C. Marcucci, C. R. Oliveira, G. J. S. Pereira, and C. Bincoletto.

2024. 'Artemisia vulgaris Induces Tumor-Selective Ferroptosis and Necroptosis via Lysosomal Ca(2+) Signaling', *Chin J Integr Med*, 30: 525-33.

Statements and Declarations

Funding: This research was funded by Fundação de Amparo a Pesquisa do Estado de São Paulo (FAPESP/Brazil, grant numbers 2019/07005-4 and 2023/01250-2 for F.W.; 2023/09878-0 for M.R.T.; 2020/15895-7 for G.R.E.; 2024/17233-2 for L.L.; 2023/15365-6 for J.L.S.S.), Conselho Nacional de Desenvolvimento Cientifico e Tecnologico (CNPq/Brazil; finance code 151318/2023-9 for M.R.T) and Coordenação de Aperfeiçoamento de Pessoal de Nível Superior (CAPES/PRINT 6685 Young Talent call 41/2017 for G.R.E; CAPES/PROBRAL; finance code 88881.895020/2023 for R.C.A. and M. B. and CAPES/PRINT; finance code 88887.979375/2024-00 for F. W.).

Conflicts of interest: The authors have no conflicts of interest to declare that are relevant to the content of this article.

Author contributions: Conceptualization, G.R.E and F.W.; methodology, G.R.E. and F.W.; formal analysis, M.R.T., G.R.E. and F.W.; investigation, M.R.T., G.R.E., L.L.; resources, F.W.; data curation, F.W.; writing—original draft preparation, M.R.T. and F.W.; writing—review and editing, M.R.T., G.R.E, L.L., J.L.S.S., R.C.A. and M.B.; visualization, M.R.T. and F.W.; supervision, F.W.; project administration, F.W.; funding acquisition, F.W. All authors have read and agreed to the published version of the manuscript.

Data Availability: The datasets generated during and/or analysed during the current study are available in the UNIFESP repository, https://repositorio.unifesp.br/

Ethics approval: This study was performed in line with the principles of the Declaration of Helsinki. Approval was granted by the Ethics Committee on the Use of Animals of the Universidade Federal de Sao Paulo (Date: 02/10/2023 No: 5501010623).

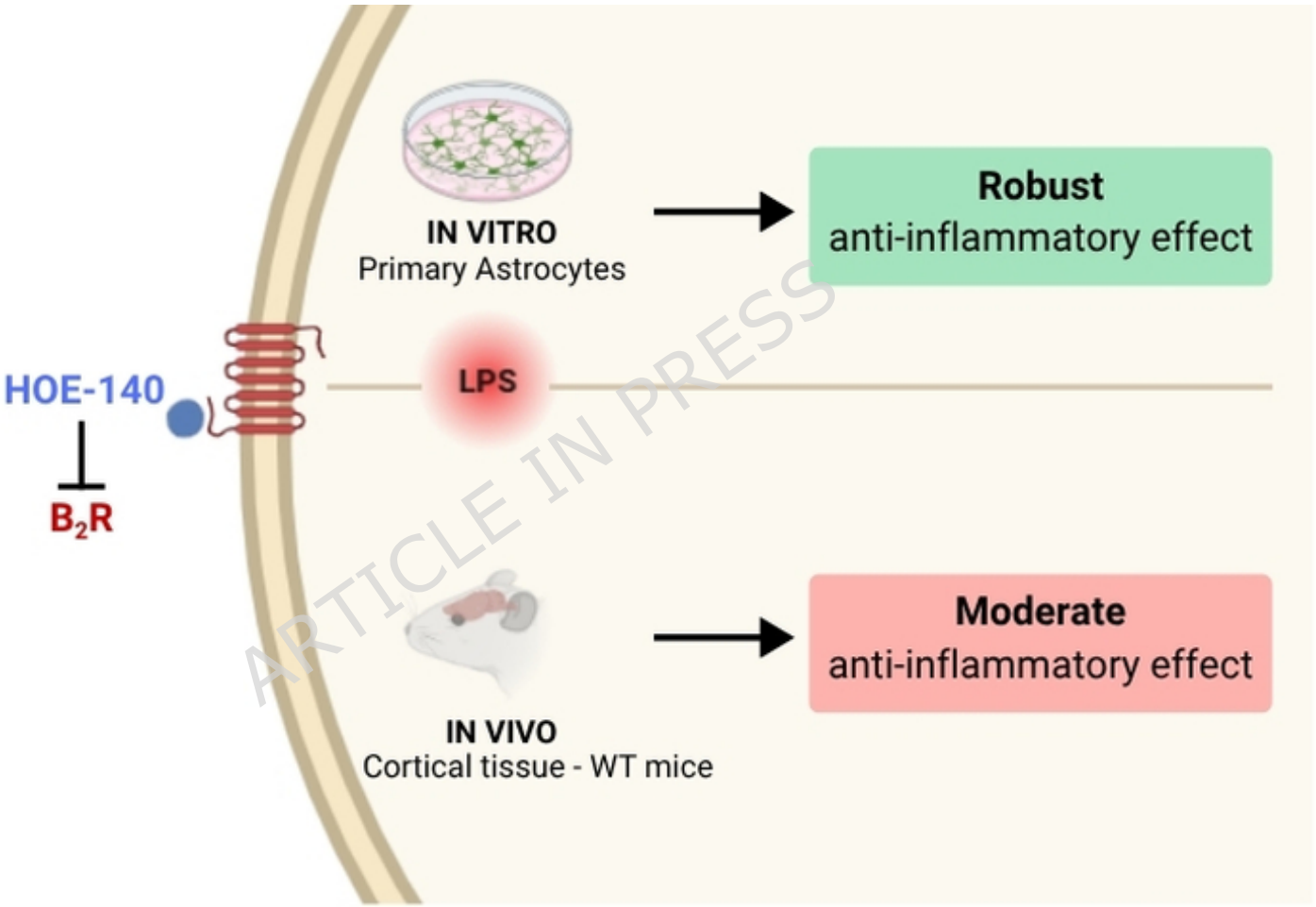

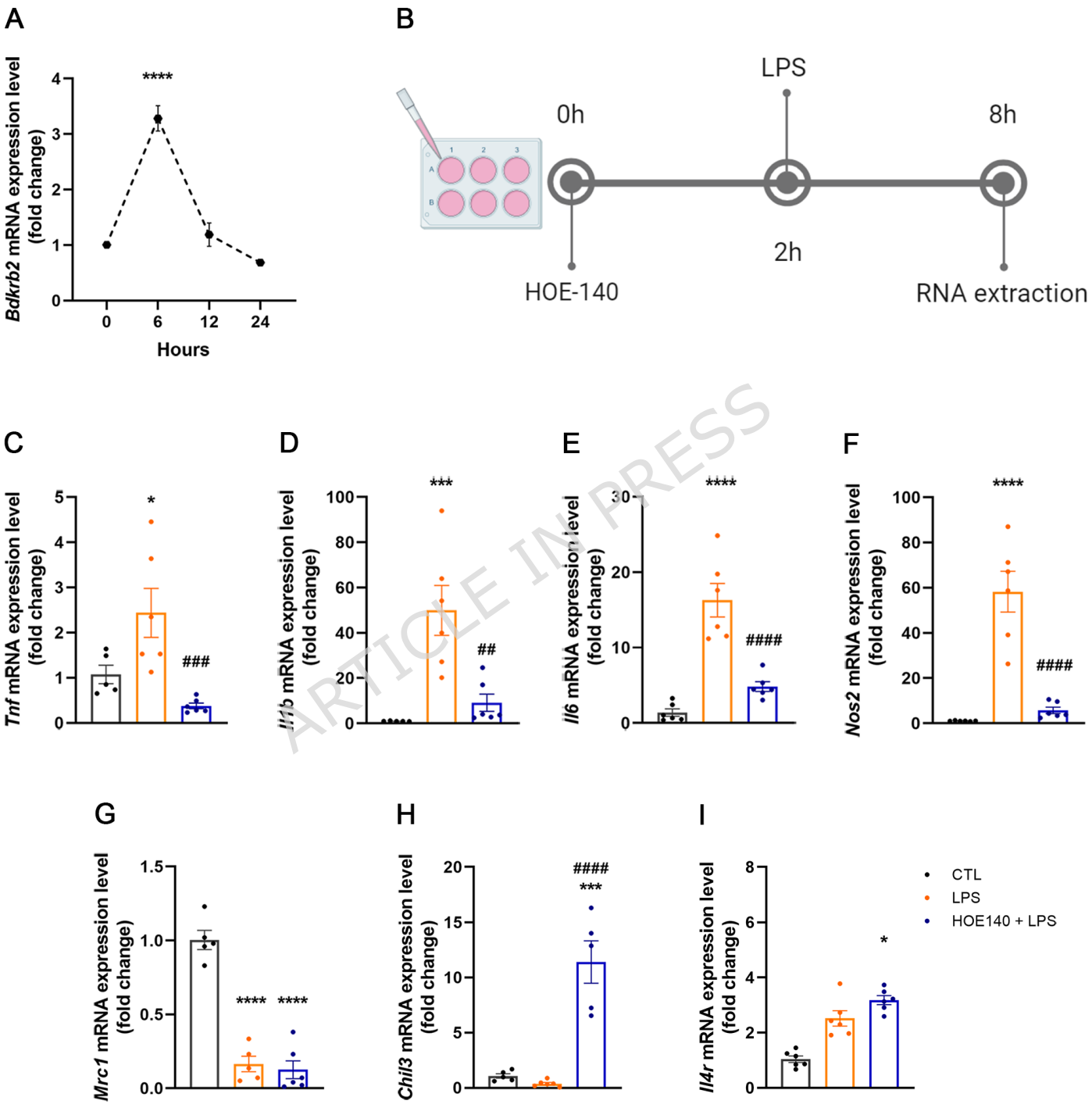

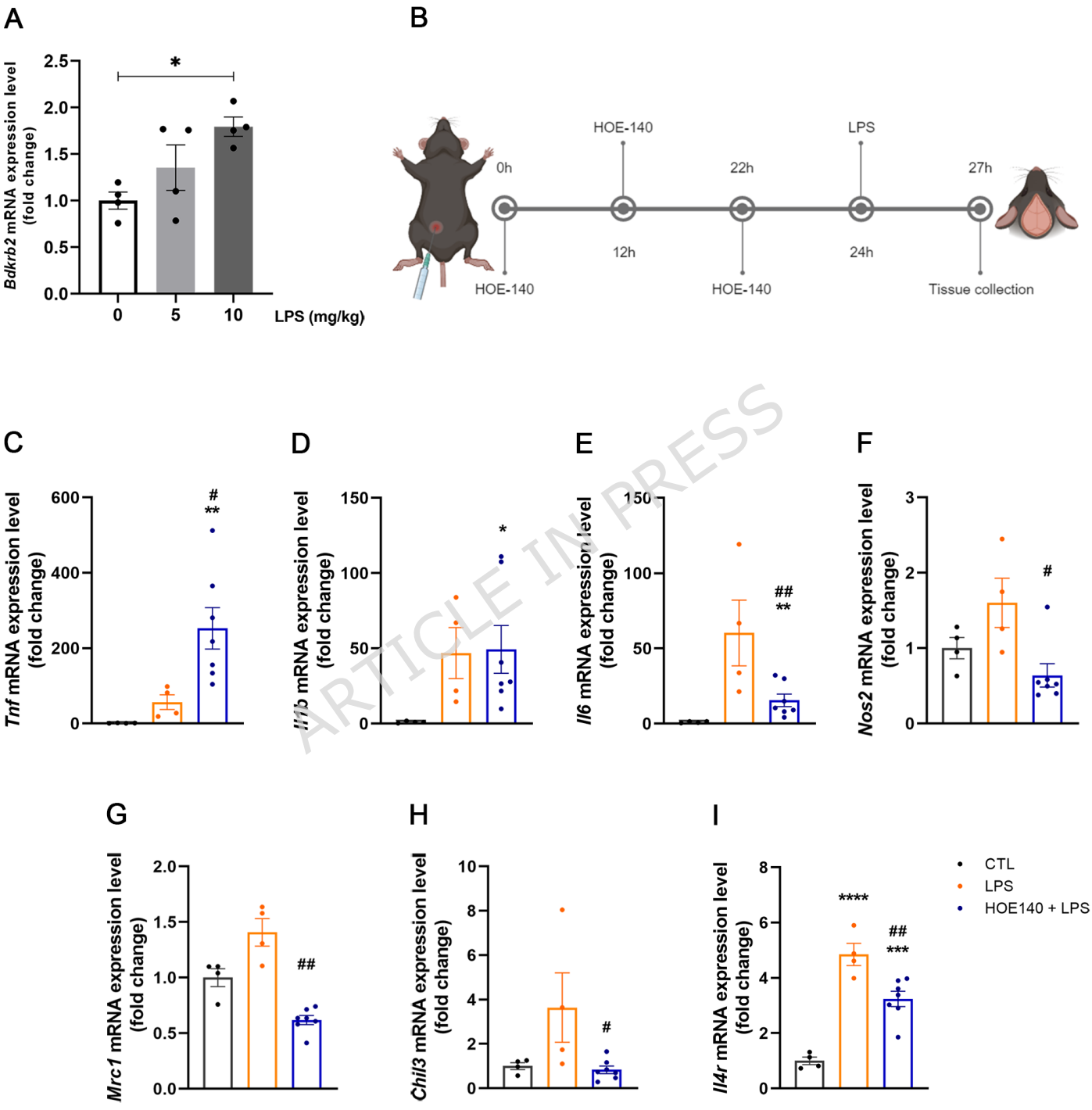

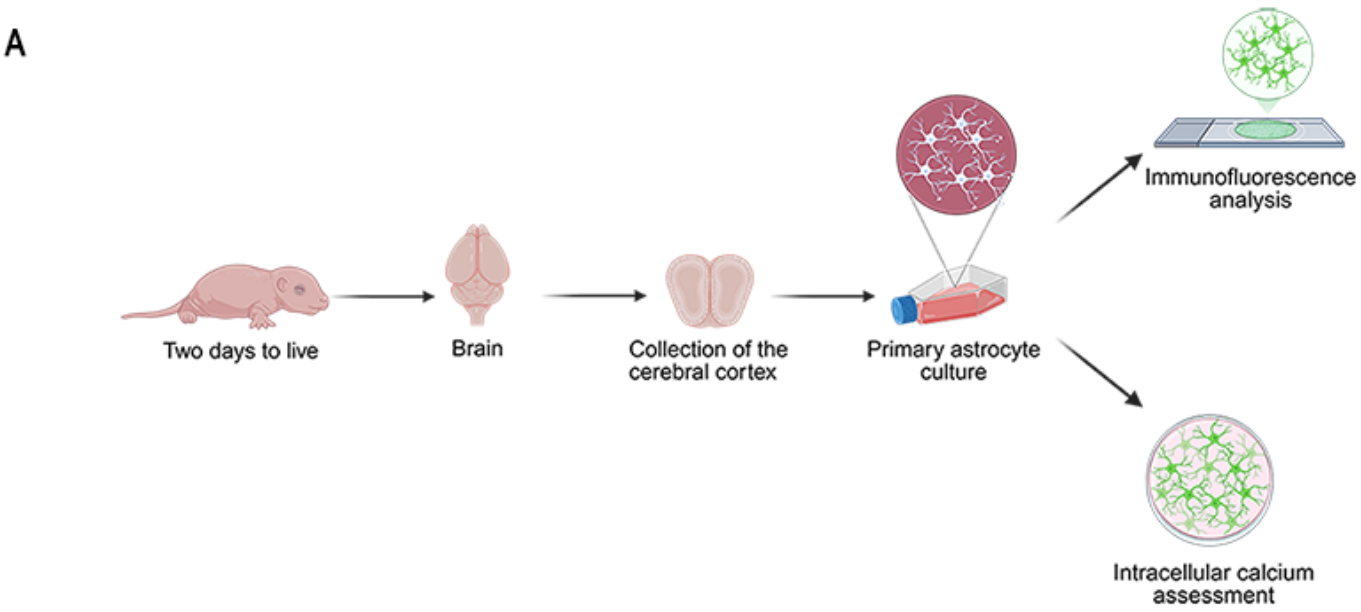

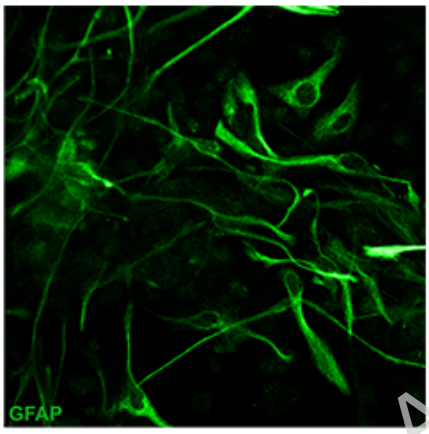

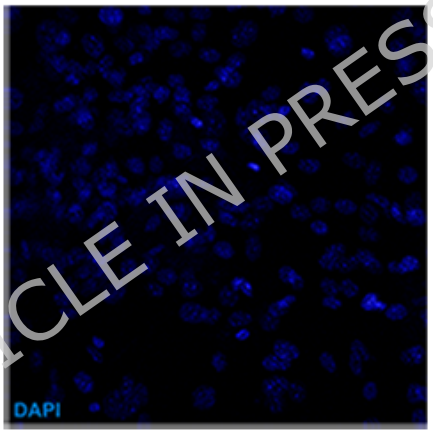

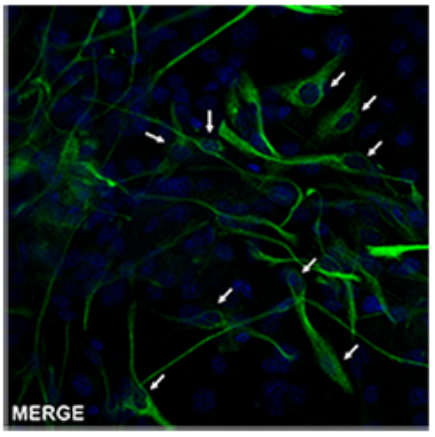

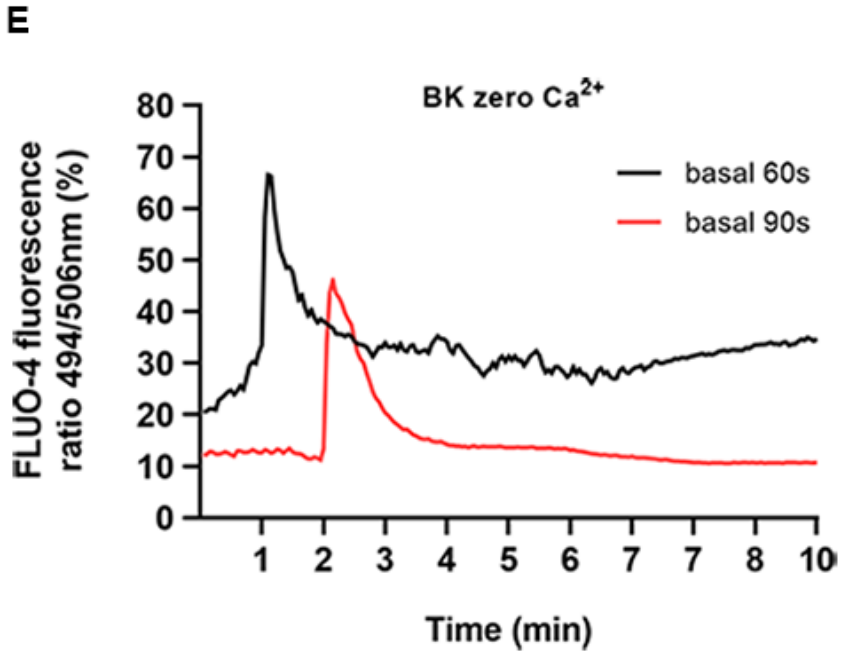

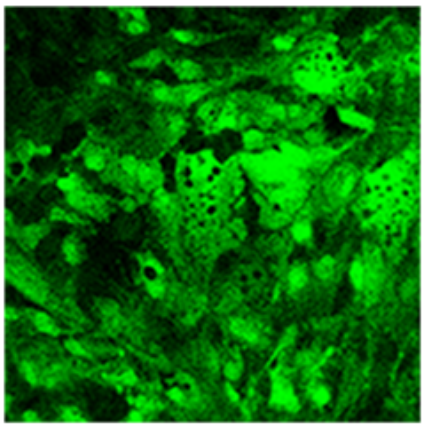

Table 1. Primer identification and sequences

Target gene	Gene function	Foward primer	Reverse primer
Actb (β-actin)	Reference gene	gctccggcatgtgcaaag	catcacaccctggtgccta
Bdkrb2 (B2R)	Bradykinin B2 receptor	ggtgctgaggaacaacgaga	cccaacacagcacaaagag
Chil3 (YM1)	M2 macrophages marker	cccctggacatggatgactt	agctcctctcaataagggcc
Gapdh	Reference gene	gctagccctggacatcgaga	ccccttctttggtgcttttgc
Il1b (IL-1β)	Proinflammatory cytokine	gccacctttgacagtgatg	atgtgctgctgcgagatttg
Il4r (IL-4R)	Antiinflammatory marker	cacagtgcacgaaagctgaa	atgggcacaagctgtggtag
Il6 (IL-6)	Proinflammatory cytokine	tagtccttcctaccccaatttcc	ttggtccttagccactcctcc
Mrc1 (CD206)	M2 macrophages marker	caaggaaggttggcatttgt	cctttcagtcctttgcaagc
Nos2 (iNOS)	Nitric oxide production	ctgctggtggtgacaagcacattt	atgtcatgagcaaaggcgc
Ppia	Reference gene	cttcttgctggtcttgccattcc	tatctgcactgccaagactg
Tnf (TNF-α)	Proinflammatory cytokine	gcctcttctcattcctgcttg	ctgatgagagggaggccat